GEOMAGNETIC PERTURBATIONS IN A STRATIFIED MEDIUM, CAUSED BY PROPAGATION OF A LONGITUDINAL SPHERICAL WAVE

V. V. Surkov

UDC 533.95:537.84

Acoustic wave propagation in Earth leads to perturbations in the geomagnetic field [1-3]. The study of electromagnetic signals provides additional information on both the seismic source and the rocky state (in particular, its electrical conductivity). In theoretical studies one consideres magnetic perturbations due to Rayleigh surface waves having the highest amplitude at large distances from the surface [4-7]. Thus, in [5] was investigated a quasiharmonic Rayleigh wave in an external magnetic field, and in [6] – perturbations due to surface waves initiated by linear and point sources.

In the present study we calculate magnetic perturbations near a source of longitudinal spherical waves for any reduced potential function of elastic displacements. We investigate the various mechanisms of appearance of an electromagnetic signal. We analyze the effect of diffusion of the generated currents, and single out the term describing local magnetic perturbations near the elastic wave front.

Consider a homogeneous elastic space with electrical conductivity σ_1 for $z < 0$ and σ_2 for $z > 0$. The medium is located in a uniform external magnetic field $\mathbf{H} = H_0\mathbf{e}_z$. A spherical longitudinal elastic wave is generated at moment of time $t = 0$ in the lower half-space, while the wave source is a spherical radiator of radius R_0, whose center is located at depth z_0 (Fig. 1).

We calculate the perturbation of the external magnetic field, caused by the motion of conducting layers of the medium in the elastic wave. Assuming that the perturbation generated is weak, i.e., $\delta H \equiv H \ll H_0$, within the quasistationary approximation we write the equations

$$\partial \mathbf{H}/\partial t = \mathrm{rot}\,[\mathbf{v}\mathbf{H}_0] + D_{1,2}\Delta\mathbf{H},\ \mathrm{div}\mathbf{H} = 0,\ D_{1,2} = (\mu_0\sigma_{1,2})^{-1}, \tag{1}$$

where $D_{1,2}$ are, respectively, the diffusion coefficients of magnetic perturbation for the lower and upper half-space. The velocity field $\mathbf{v}$ is assumed to be a known function of coordinates and of time. Taking into account the axial symmetry of the problem, we use a cylindrical coordinate system z, r with center at the point 0. Equations (1) acquire in this case the form

$$\frac{\partial H_r}{\partial t} = D_{1,2}\left[\frac{1}{r}\frac{\partial}{\partial r}\left(r\frac{\partial H_r}{\partial r}\right) - \frac{H_r}{r^2} + \frac{\partial^2 H_r}{\partial z^2}\right] + H_0\frac{\partial v_r}{\partial z}; \tag{2}$$

$$\frac{\partial H_z}{\partial t} = D_{1,2}\left[\frac{1}{r}\frac{\partial}{\partial r}\left(r\frac{\partial H_z}{\partial r}\right) + \frac{\partial^2 H_z}{\partial z^2}\right] + \frac{H_0}{r}\frac{\partial}{\partial r}rv_r; \tag{3}$$

$$\frac{1}{r}\frac{\partial}{\partial r}(rH_r) + \frac{\partial H_z}{\partial z} = 0 \tag{4}$$

(v_r is the projection of the radial velocity of the medium on the polar radius r). In a longitudinal spherical wave v_r is expressed in terms of the reduced displacement potential $f(\xi)$:

$$v_r = \frac{c_l R_0 r}{R^2}\left(\ddot{f} + \frac{R_0}{R}\dot{f}\right),\quad R = \sqrt{r^2 + (z+z_0)^2}\ \ (R_0 < R < R_* = R_0 + c_l t). \tag{5}$$

Here $\xi = (c_\ell t - R)/R_0 + 1$, c_ℓ is the velocity of longitudinal elastic wave, and the dot denotes differentiation with respect to ξ. The shape of the function f is determined by the boundary conditions on the surface of the elastic radiator and at the front of the longitudinal wave. In what follows it is assumed that the elastic properties of both media are identical, thus excluding from treatment the wave field reflected from the wave boundary.

Moscow. Translated from Zhurnal Prikladnoi Mekhaniki i Tekhnicheskoi Fiziki, No. 5, pp. 20-30, September-October, 1989. Original article submitted April 21, 1988.

0021-8944/89/3005-0687$12.50

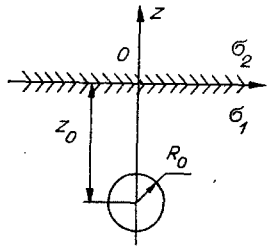

Fig. 1

The contribution of reflected elastic waves to magnetic perturbations can be accounted for separately.

We apply the Fourier transform to Eqs. (2)-(4). We note that the Fourier component (5) can be represented as ($R \geq R_0$)

$$\tilde{v}_r = \int_{-\infty}^{\infty} v_r e^{i\omega t}\, dt = A(k)\frac{\partial}{\partial r}\frac{e^{ikR}}{R}, \quad A(k) = -R_0^3 \int_0^{\infty} \dot{f}(\eta)\, e^{ikR_0(\eta-1)}\, d\eta \tag{6}$$

($k = \omega/c_\ell$). In expressions (6) we can use the well-known Weyl representation

$$\frac{e^{ikR}}{R} = \frac{ik}{2}\int_{-\infty}^{\infty} H_0^{(1)}(krq)\exp\left[ik\,|z+z_0|\sqrt{1-q^2}\right]\frac{q\,dq}{\sqrt{1-q^2}}, \tag{7}$$

where $H_0^{(1)}$ is the Hankel function of the first kind, and $\arg\sqrt{1-q^2} = \pi/2$ for $q > 1$. Taking into account the shape of expression (7), we seek the Fourier components of the magnetic perturbations in the form

$$\tilde{H}_r = \int_{-\infty}^{\infty} h_r(z, q, k) H_1^{(1)}(krq)\, dq, \quad \tilde{H}_z = \int_{-\infty}^{\infty} h_z(z, q, k) H_0^{(1)}(krq)\, dq. \tag{8}$$

Substituting (6)-(8) into (2)-(4), we obtain a system of equations, among which the following are independent:

$$h_z'' - \varkappa_{1,2}^2 h_z = -\frac{H_0 A(k) k^4 q^3}{2bD_{1,2}} e^{b|z+z_0|}, \quad b = ik\sqrt{1-q^2}; \tag{9}$$

$$h_z' + qkh_r = 0, \quad \varkappa_{1,2} = \sqrt{q^2k^2 - ikk_{1,2}}, \quad k_{1,2} = c_l/D_{1,2} \tag{10}$$

(the prime denotes differentiation with respect to z). The functions h_z, h_r must be continuous at $z = 0$ and $z = -z_0$. Also requiring that h_z and h_r tend to zero for $|z| \to \infty$, we find the solution of (9), (10):

$$\begin{aligned} h_z &= C_1 e^{\varkappa_1 z} + a_1 e^{-b(z+z_0)} && (z < -z_0), \\ h_z &= C_2 e^{\varkappa_1 z} + C_3 e^{-\varkappa_1 z} + a_1 e^{b(z+z_0)} && (-z_0 < z < 0), \\ h_z &= C_4 e^{-\varkappa_2 z} + a_2 e^{b(z+z_0)} && (z > 0). \end{aligned} \tag{11}$$

The function h_r can be determined from (11) by means of (10). Here we used the notation

$$C_1 = C_2 + \frac{ba_1}{\varkappa_1} e^{\varkappa_1 z_0}, \quad C_2 = \frac{ba_1(\varkappa_1 - \varkappa_2)}{\varkappa_1(\varkappa_1 + \varkappa_2)} e^{-\varkappa_1 z_0} + \frac{(a_2 - a_1)(b + \varkappa_2)}{\varkappa_1 + \varkappa_2} e^{bz_0}, \tag{12}$$

$$C_3 = \frac{ba_1}{\varkappa_1} e^{-\varkappa_1 z_0}, \quad C_4 = \frac{2ba_1}{\varkappa_1 + \varkappa_2} e^{-\varkappa_1 z_0} + \frac{(a_1 - a_2)(\varkappa_1 - b)}{\varkappa_1 + \varkappa_2} e^{bz_0}, \quad a_{1,2} = \frac{H_0 A(k) k^3 q^3}{2D_{1,2} b(k - ik_1)},$$

while on the real axis $\mathrm{Re}\,\varkappa_{1,2} > 0$. Substituting (11), (12) into (8), we have a solution of the problem in the Fourier representation.

The integrals (8) are calculated approximately for large distances r, using the asymptotic expression for the Hankel function for $kr \gg 1$. For $z \geq 0$, we obtain the expressions

$$\tilde{H}_z = \frac{Bk^{5/2}}{\sqrt{2\pi r}} \int_{-\infty}^{\infty} F(z, k, q)\, dq, \quad \tilde{H}_r = \frac{iBk^{3/2}}{\sqrt{2\pi r}} \int_{-\infty}^{\infty} \frac{dF(z, k, q)}{dz}\frac{dq}{q}, \quad B = \frac{H_0 A}{D_1},$$

$$F=\left\{\left[2e^{-\varkappa_1 z_0}+\frac{k(k_1-k_2)(\varkappa_1-b)}{k_1(k-ik_2)b}e^{bz_0}\right]\frac{e^{-\varkappa_2 z}}{(k-ik_1)(\varkappa_1+\varkappa_2)}+\right. \tag{13}$$
$$\left.+\frac{k_2 e^{b(z+z_0)}}{k_1(k-ik_2)b}\right\}q^{5/2}e^{ikrq-\pi i/4}.$$

Consider the case $k_1 > k_2$. For $k > 0$ we carry out cuts in the complex q plane from the branching points of the roots of the expressions: $\pm q_1 = (ik_1/k)^{1/2}$, $\pm q_2 = (ik_2/k)^{1/2}$, $\pm q_3 = 1$, as is shown in Fig. 2. Then $\mathrm{Re}\varkappa_{1,2} > 0$ everywhere, except for the sectors confined by the cut-off lines c_1, c_2 and by the dashed lines. The range of values of the variable q, where $\mathrm{Re}b < 0$, is confined by the branch cut c_3 and the dashed-dotted line.

We investigate the function $\tilde{H}_z$ for $z_0 = 0$. Equation (13) contains exponents of the functions $f_1 = ikrq - \varkappa_2 z$ and $f_2 = ikrq + bz$, having extrema at the points $q_4 = (ik_2/k)^{1/2}r/R$ and $q_5 = r/R$, respectively, located on the selected branch of the Riemann surface. We place the integration contour in the upper half-plane, so that it passes through the saddle points in the directions $\theta_4 = -\pi/8$, $\theta_5 = -\pi/4$ (curve 1 of Fig. 2). Denoting by $\tilde{H}_1$ the integral calculated along this path by the steepest descent method, we find the approximate expression

$$\tilde{H}_1=\frac{Br^2}{R^3}\left\{\frac{ik_2^{3/2}z\exp\left(-R\sqrt{-ikk_2}\right)}{r(k-ik_1)\left(\sqrt{k_1R^2/r^2-k_2}+\sqrt{k_2}z/r\right)}\left[2-\frac{k(k_1-k_2)}{k_1(k-ik_2)}\times\right.\right. \tag{14}$$
$$\left.\left.\times\left(e^{\pi i/4}\sqrt{\frac{k_1R^2/r^2-k_2}{kR^2/r^2-ik_2}}+1\right)\right]-\frac{kk_2}{k_1(k-ik_2)}e^{ikR}\right\},\quad R=\sqrt{r^2+z^2}.$$

Here the last term determines the contribution of the neighborhood of the point q_5, while the remaining terms are due to the neighborhood of the point q_4.

In the case $z = 0$ the exponents in (13) of the functions $f_3 = ikrq - \varkappa_1 z_0$ and $f_4 = ikrq + bz_0$ have extrema at the points $q_6 = (ik_1/k)^{1/2}r/R$ and $q_7 = r/R$ ($R = \sqrt{r^2+z_0^2}$). Deforming the integration contour so that it passes through the saddle points $\theta_6 = -\pi/8$ and $\theta_7 = -\pi/4$ (path 2 in Fig. 2), we obtain

$$\tilde{H}_2=\frac{Br^2}{R^3}\left\{\frac{2z_0k_1^{3/2}\exp\left(-R\sqrt{-ikk_1}\right)}{r\left(\sqrt{k_1-k_2R^2/r^2}-i\sqrt{k_1}z_0/r\right)(k-ik_1)}-\frac{kk_2}{k_1(k-ik_2)}e^{ikR}\times\right. \tag{15}$$
$$\left.\times\left(1+\frac{k(k_1-k_2)}{k_2(k-ik_1)}\left[\frac{\sqrt{k-ik_1R^2/r^2}-i\sqrt{k}z_0/r}{\sqrt{k-ik_1R^2/r^2}+\sqrt{k-ik_2R^2/r^2}}\right]\right)\right\},\quad R=\sqrt{r^2+z_0^2},$$

where it is assumed that $k_1 > k_2R^2/r^2$. The first term in (15) is related to the neighborhood of the point q_6, and the second is due to the point q_7. If $k_2 \neq 0$, (15) must be supplemented by the term (18), related to the bypass of the branch cut c_2.

Equations (14) and (15) are not valid for $z, z_0 \to 0$, since in this case the saddle points q_4-q_7 approach the branching points q_1, q_2, q_3. We investigate this case separately, putting $z = z_0 = 0$. We deform the original contour from above in such a manner that the integration is carried out along branch cuts (curve 3 of Fig. 2). Since, besides branch points, there are no other singularities in the q-plane in the integrand expression, the integral as a whole reduces to contributions of branch cuts. We parametrize the branch cuts $c_{1,2}$ in the form $\sqrt{q^2-q_{1,2}^2} = p\exp(3\pi i/8)$, where p is a real variable, while on the left-hand shores $p < 0$, and on the right-hand ones $p > 0$. Transforming in $\tilde{H}_z$ (13) to the variable p and transforming the integral to the interval $0, \infty$, after several transformations we obtain an expression determining the contribution of the branch cut c_2:

$$\tilde{H}_{c_2}=\frac{2Bk^{5/2}}{\sqrt{2\pi r}(k_1-k_2)(k-ik_1)}\int_0^\infty\left[2+\frac{k(k_1-k_2)(\varkappa_1-b)}{k_1b(k-ik_2)}\right]\times \tag{16}$$
$$\times q^{3/2}p^2\exp\left(ikrq+\frac{3\pi i}{8}\right)dp,$$
$$q=\left[q_2^2+p^2\exp\frac{3\pi i}{4}\right]^{1/2},\quad b=ik\left[1-q_2^2-p^2\exp\frac{3\pi i}{4}\right]^{1/2},$$
$$\varkappa_1=k\left[p^2\exp\frac{3\pi i}{4}-\frac{i(k_1-k_2)}{k}\right]^{1/2}.$$

While for $p < p_0 = [\sqrt{2}(k_1 - k_2)/k]^{1/2}$ (the region below the upper primed line in Fig. 2) $\mathrm{Re}\varkappa_1 > 0$, for $p > p_0$ $\mathrm{Re}\varkappa_1 < 0$. At the saddle point $p = 0$ the pre-exponential factor in (16)

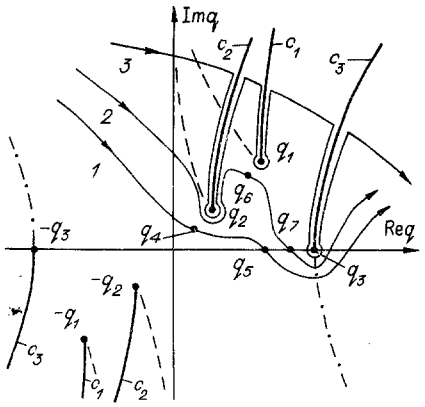

Fig. 2

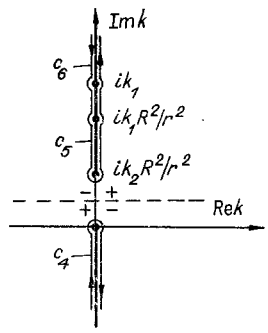

Fig. 3

vanishes; therefore we seek an extremum of the function f = ikrq(p) + 2 lnp. For kr $\gg$ 1, the saddle point is $p_* = (2/kr)^{1/2}(k_2/k)^{1/4}$. Expending f(p) in the neighborhood of this point, we have

$$\exp f(p) \approx \frac{2}{kr}\sqrt{\frac{k_2}{k}}\exp\left[-r\sqrt{kk_2}\left\{\frac{1-i}{\sqrt{2}}+\frac{k}{k_2}(p-p_*)^2\right\}\right]. \tag{17}$$

Substituting (17) into (16) and integrating over the real variable p, we find

$$\tilde{H}_{c_2} = \frac{Bk_2^{3/2}\sqrt{2}}{r^2(k_1-k_2)(k-ik_1)\sqrt{k}}\left[2-\frac{k(k_1-k_2)}{k_1(k-ik_2)}\left(e^{\pi i/4}\sqrt{\frac{k_1-k_2}{k-i(k_2+\alpha_2)}}+\right.\right.$$
$$\left.\left.+1\right)\right]\exp\left(-r\sqrt{-ikk_2}+\frac{3\pi i}{4}\right),\quad \alpha_2 = \frac{2}{r}\left(\frac{k_2}{k}\right)^{1/2}e^{\pi i/4}. \tag{18}$$

Following similar calculations we determine the contribution of the branch cut c_1:

$$\tilde{H}_{c_1} = -\frac{Bk_1^{3/2}\sqrt{2}}{r^2(k_1-k_2)(k-ik_1)\sqrt{k}}\left[2-\frac{k(k_1-k_2)}{k_1(k-ik_2)}\times\right.$$
$$\left.\times\left(e^{-\pi i/4}\sqrt{\frac{k_1-k_2}{k-i(k_1+\alpha_1)}}+1\right)\right]\exp\left(-r\sqrt{-ikk_1}+\frac{3\pi i}{4}\right), \tag{19}$$
$$\alpha_1 = \frac{2}{r}\left(\frac{k_1}{k}\right)^{1/2}e^{\pi i/4}.$$

The branch cut c_3 is parametrized in the form $i\sqrt{1-q^2} = -p\exp(\pi i/4)$, while on the left shore of the branch cut p < 0, and on the right one p > 0. Transforming in (13) to the variable p, and transforming the integral to the segment 0, ∞, we obtain

$$\tilde{H}_{c_3} = -\frac{2Bk_2k^{3/2}}{\sqrt{2\pi r}(k-ik_2)k_1}\int_0^\infty\left[1+\frac{k(k_1-k_2)\varkappa_1}{k_2(k-ik_1)(\varkappa_1+\varkappa_2)}\right]q^{3/2}e^{ikrq}\,dp, \tag{20}$$

where $q = (1+ip^2)^{1/2}$, $\varkappa_{1,2} = k(1-q_{1,2}^2+ip^2)^{1/2}$, while $\mathrm{Re}\,\varkappa_{1,2} > 0$. Near the saddle point p = 0 the exponent acquires the form $ikr \approx kr(i-p^2/2)$. Substituting this relation into (20), and putting in the pre-exponential factor p = 0, we have after integration

$$\tilde{H}_{c_3} = -\frac{Bkk_2}{rk_1(k-ik_2)}\left\{1+\frac{k(k_1-k_2)}{k_2\sqrt{k-ik_1}\left(\sqrt{k-ik_1}+\sqrt{k-ik_2}\right)}\right\}e^{ikr}. \tag{21}$$

Thus, for the given case the solution is $\tilde{H}_3 = \tilde{H}_{c_1} + \tilde{H}_{c_2} + \tilde{H}_{c_3}$ [the terms are determined by Eqs. (18), (19), (21)]. We note that for z, $z_0 \to 0$ in relations (14) and (15), only those terms survive which transform to the limit in expression (21).

Taking into account that k > 0 was considered above, we use the equation of the inverse Fourier transform

$$H_z = \frac{c_l}{\pi}\,\mathrm{Re}\int_0^\infty \tilde{H}_z(k)\,e^{-ikc_lt}\,dk, \tag{22}$$

We carry out cuts in the complex k-plane in such a manner that the condition $\mathrm{Re}\varkappa_{1,2} = \mathrm{Re}[k(k - ik_{1,2}R^2/r^2)]^{1/2} > 0$ is satisfied everywhere. These branch cuts are denoted in Fig. 3 by c_4, c_5 (up to the point $k = ik_1R^2/r^2$), and c_6. On the lines $\mathrm{Re}k = 0$ and $k = ik_2R^2/2r^2$, denoted by dashes, $\mathrm{Im}\varkappa_2 = 0$. The signs of $\mathrm{Im}\varkappa_2$ are indicated in Fig. 3. Similarly the lines $\mathrm{Re}k = 0$ and $k = ik_1R^2/2r^2$ determine the sign-varying regions of $\mathrm{Im}\varkappa_1$.

Consider initially relation (15) (for $z = 0$, $z_0 \neq 0$). We substitute it in (22) with account of the expression for A(k) from (16). Transforming part of the terms to the integration interval $k - \infty$, ∞, we obtain

$$H_2 = H_d + H_e, \quad H_d = -\frac{2Qz_0r^3k_1^{5/2}}{(k_1-k_2)R^2}\int_0^\infty \dot{f}(\eta)\,d\eta\left\{\sqrt{k_1 - k_2\frac{R^2}{r^2}}\times\right. \tag{23}$$

$$\left.\times\,\mathrm{Re}\int_0^\infty \frac{\exp\left(-R\sqrt{-ikk_1}-ikL\right)}{k-ik_1}\,dk + \sqrt{k_1}\,\frac{zi}{2r}\int_{-\infty}^{\infty}\frac{\exp\left(-R\sqrt{-ikk_1}-ikL\right)}{k-ik_1}\,dk\right\},$$

$$H_e = \frac{Qk_2r^2}{2}\int_{-\infty}^{\infty}\left\{\left[\frac{\sqrt{k-ik_1R^2/r^2}-i\sqrt{k}\,z_0r}{\sqrt{k-ik_1R^2/r^2}+\sqrt{k-ik_2R^2/r^2}}\right]\frac{k(k_1-k_2)}{k_2(k-ik_1)}+1\right\}\frac{k\,dk}{k-ik_2}\times$$

$$\times\int_0^\infty \dot{f}(\eta)\,e^{ikR_0(\eta-\xi)}\,d\eta, \quad Q = \frac{H_0R_0^3}{\pi R^3}, \quad L = R_* - R_0\eta.$$

Here it was taken into account that the integral over η converges absolutely, and therefore in H_d one changes the order of integration over η and k. In H_e and for $\xi > 0$ the replacement of integrals is not allowed, since the integral over k diverges for $\eta = \xi$.

Investigate the term H_d. If the function $\dot{f}(\eta)$ decreases sufficiently quickly, so that the basic contribution to the integral over η is related to the region $\eta < R_*/R_0$, then $L > 0$ in the integral over k. The integration contour must be closed from below. In this case the integration in the first term is carried out over the right-hand shore, and in the second – over both shores of the branch cut c_4. Following the variable replacement $k = -ix^2/(k_1R^2)$

$$H_d = \frac{4Qk_1^3r^3z_0}{(k_1-k_2)R^2}\int_0^{R_*}\dot{f}(\eta)\,d\eta\int_0^\infty\left(\frac{z_0}{r}\sin x - \right. \tag{24}$$

$$\left. - \sqrt{1-\frac{k_2R^2}{k_1r^2}}\cos x\right)\frac{x\exp\left(-\dfrac{x^2L}{k_1R^2}\right)}{x^2+k_1^2R^2}\,dx.$$

We transform the integral of the second term in (24)

$$\int_0^\infty \frac{x\cos x}{x^2+k_1^2R^2}\exp\left(-\frac{x^2L}{k_1R^2}\right)dx = \int_0^\infty \Phi\left(x+\frac{L}{k_1R^2}\right)e^{-xk_1^2R^2}\,dx, \tag{25}$$

$$\Phi(y) = \frac{1}{2y}\left[1 - \frac{1}{\sqrt{y}}\exp\left(-\frac{1}{4y}\right)\int_0^{1/2\sqrt{y}} e^{x'^2}\,dx'\right].$$

If $k_1^2R^2 \gg 1$, one can put in the functions $\Phi x \approx 0$. The first integral over x in (24) is calculated accurately, therefore the final result is

$$H_d = \frac{H_0R_0^3k_1rz_0}{(k_1-k_2)R^5}\int_0^{R_*}\dot{f}(\eta)\left\{k_1^2rz_0\,e^{k_1L}\left[e^{k_1R}\,\mathrm{erfc}\left(\sqrt{k_1L}+\frac{R}{2}\sqrt{\frac{k_1}{L}}\right)-\right.\right. \tag{26}$$

$$\left.\left. - e^{-k_1R}\,\mathrm{erfc}\left(\sqrt{k_1L}-\frac{R}{2}\sqrt{\frac{k_1}{L}}\right)\right] - \frac{4r^2}{\pi R^2}\sqrt{1-\frac{k_2R^2}{k_1r^2}}\,\Phi\left(\frac{L}{k_1R^2}\right)\right\}d\eta.$$

The structure of expression (26) shows that it describes diffusion processes of currents and magnetic perturbations, generated behind the front of the shock wave. Thus, for a source of the delta-function type and under the conditions $R_* \gg R$, k_1^{-1} the expression in the square brackets in (26) is written as $-R\exp(-k_1R^2/4R_*)/2R_*\sqrt{\pi}$. It is hence seen that the given term is substantial in the region $R \lesssim \sqrt{Dt}$, where the effect of diffusion perturbations, generated initially in the neighborhood $R \sim R_0$, is noticeable. At large distances, if $R \gg R_*$, k_1^{-1}, the given expression has the asymptotic form $-\exp(k_1R_0\xi)$. Here the basic role is played by perturbations originating from the front of the elastic wave, where the quasistationary (without account of the geometric factor) running pattern is formed.

The last term in (26) decreases at large distances as a power law (since for $R \to \infty$, $\Phi \to -1$), indicating the magnetic dipole character of the given term. The effective magnetic moment is due to the sign-varying currents, lumped in the region $R \lesssim R_*$.

The term H_e is investigated in the region $\xi < 0$, putting for simplicity $z_0 = 0$. Changing the order of integration over η and k, we deform the integration contour to the branch cut c_5. Taking into account that the integrand has no singularity at the point $k = ik_2$, we obtain

$$H_e = -\frac{H_0 R_0^3}{\pi r}\int_0^\infty \dot{f}(\eta)\, e^{-k_2 R_0(\eta+|\xi|)}\, d\eta \int_0^{k_1-k_2} \frac{(k_2+p)^2}{\sqrt{p(k_1-k_2-p)}}\, e^{-pR_0(\eta+|\xi|)}\, dp. \tag{27}$$

Calculating the internal integral, we reach the relation

$$H_e = \frac{H_0 R_0^2}{2r}\, e^{-k_2 R_0|\xi|}\int_0^\infty \dot{f}(\eta)\, e^{-k_2 R_0 \eta}\, \frac{d}{d\eta}\left[(k_1+k_2) I_0(s) - (k_1-k_2) I_1(s)\right] d\eta, \tag{28}$$

$$s = (k_1 - k_2) R_0 (\eta + |\xi|)/2,$$

where I_0, I_1 are the modified Bessel functions of the first kind. It is hence seen that the term H_e describes perturbations localized near the front ($\xi = 0$) of the elastic wave. Their amplitude decreases with distance by the same law as the velocity amplitude of the medium $\sim r^{-1}$. Far from the front of the longitudinal wave, if $k_1 R_0 |\xi| \gg 1$ and $k_2 = 0$, Eq. (28) acquires the asymptotic form

$$H_e = \frac{3H_0}{4r|\xi|^{5/2}}\sqrt{\frac{R_0}{\pi k_1}}\left[-f(\infty) + \frac{5}{2|\xi|}\int_0^\infty \eta f(\eta)\, d\eta\right]. \tag{29}$$

If there exist no residual displacements, then $f(\infty) = 0$. At large distances $|\xi| \approx r$, implying that (29) is, as is the last term in (26), the quasistatic field of some effective magnetic moment.

Similarly one can study the general expressions of H_z and H_r for other special cases ($z = 0$, $z = z_0 = 0$, and others) for an arbitrary (nondecreasing) function $f(\xi)$. However, from the analysis above it is clear that at large distances the magnetic perturbations decrease as a power law. Their highest value is achieved near the front of the elastic wave, decreasing with distance as $\sim r^{-1}$. As to diffusion processes, they can play a decisive role at the initial phase of the process, when the diffusion front $R_d \sim \sqrt{Dt}$ is ahead of the elastic wave, having size $\sim c_l t$. At distances $R \sim k_1^{-1}$ the elastic wave emerges ahead, and diffusion of the generated magnetic perturbations can predominate only near the source.

Consider as an example the magnetic field due to radiation of an elastic wave from an explosive source. At the boundary of the destruction zone of the medium, at $R = R_0$, we assign the radial component σ_{rr} of the stress tensor in the form

$$\sigma_{rr} = -[P_0 + (P_* - P_0)\exp(-t/\tau_0)]. \tag{30}$$

Here P_* is the amplitude of elastic stresses at the boundary of the destruction zone (of the order of the limiting rock strength at destruction), P_0 is a constant of the order of the lithostatic pressure, and τ_0 is the characteristic time of detonation evolution. The solution of the corresponding problem of elasticity theory under the conditions $f(0) = \dot{f}(0) = 0$ at the wave front makes it possible to find an explicit expression for the function

$$f(\xi) = a + be^{-\alpha\xi} - e^{-2\gamma\xi}\left[(a+b)\cos\delta\xi + \{2\gamma(a+b) - \alpha b\}\sin(\delta\xi)/\delta\right],$$

$$a = \frac{P_0}{4\gamma\rho c_l^2},\quad b = \frac{P_* - P_0}{\rho c_l^2(\alpha^2 - 4\gamma\alpha + 4\gamma)},\quad \gamma = \frac{c_t^2}{c_l^2},\quad \alpha = \frac{R_0}{c_l\tau_0},\quad \delta = 2\sqrt{\gamma(1-\gamma)} \tag{31}$$

(ρ is the medium density, and c_t is the velocity of transverse elastic waves). Using (31), we obtain

$$G(k) = \int_0^\infty \dot{f}(\eta)\, e^{ikR_0\eta}\, d\eta = \frac{\alpha b}{ikR_0 - \alpha} + \frac{ci - \alpha b}{2(ikR_0 + i\delta - 2\gamma)} - \frac{ci + \alpha b}{2(ikR_0 - i\delta - 2\gamma)}, \tag{32}$$

$$c = 2\gamma[2(a+b) - \alpha b]/\delta.$$

We elaborate on the case in which medium 2 is a vacuum. In Eqs. (3) and (4) the terms describing the field of elastic velocities in medium 2 vanish automatically in this case,

since $D_2 \to \infty$. The velocity field in the elastic wave, reflected from the boundary with vacuum, requires special treatment and is not accounted for here. We also restrict ourselves to calculating the stress component of the magnetic field H_z for $z_0^2/r^2 \ll 1$. Expanding H_e in (23) in the parameter z_0/r, we have

$$H_e = \frac{H_0 R_0^3 i}{2\pi r} \int_{-\infty}^{\infty} kG(k)\, e^{-ikR_0\xi} \left\{1 - \sqrt{\frac{\overline{k-ik_2}}{\overline{k-ik_1}}} - \frac{z_0 i}{r} \frac{\left(\sqrt{\overline{k-ik_1}} - \sqrt{\overline{k-ik_2}}\right)}{k-ik_1}\right\} dk. \tag{33}$$

The parameter k_2 is retained in the radical expressions for determining their signs during bypass of the branching point. For $\xi > 0$ the integration contour is closed from below. In the vanishing approximation (33) reduces to the residues at the poles $k = -i\alpha/R_0$, $k = -(2\gamma i \pm \delta)/R_0$, since the integral over the shores of the branch cut c_4 of the first two terms in (33) vanishes. The residue at the pole $k = -i\alpha/R_0$ of the last term in (33) vanishes, since the corresponding term has different signs on the shores of the branch cut c_4. The contribution of this term is determined by the remaining poles and the bypass of the branch cut.

As a result of the calculation we find

$$H_e = \frac{H_0 R_0}{r}\left\{\alpha^2 b\left(\sqrt{\frac{\alpha}{\alpha + k_1 R_0}} - 1\right) e^{-\alpha\xi} + \right. \tag{34}$$

$$+ \operatorname{Re}\left[\frac{(c - \alpha b i)(\delta - 2\gamma i)}{\exp\{\xi(2\gamma + i\delta)\}}\left(\sqrt{\frac{\delta - 2\gamma i}{\delta - i(2\gamma + k_1 R_0)}} - 1\right)\right] +$$

$$\left. + \frac{z_0}{r}\left(\operatorname{Re}\left[\frac{\left(\sqrt{\delta - i(2\gamma + k_1 R_0)} - \sqrt{\delta - 2\gamma i}\right)(\delta - 2\gamma i)^{3/2}(a + bi)}{\{\delta - i(2\gamma + k_1 R_0)\}\exp\{\xi(2\gamma + i\delta)\}}\right] + B_0\right)\right\},$$

$$B_0 = \frac{k_1^2 R_0^2}{\pi}\,\text{v.p.}\int_0^{\infty} \frac{x^{3/2} g(-x)\exp(-k_1 R_0 \xi x)}{(\sqrt{1+x} + \sqrt{x})(1+x)}\, dx,$$

$$g(x) = \frac{\alpha b}{\alpha + x k_1 R_0} - \frac{4\gamma(a+b) + x k_1 R_0 \alpha b}{(x k_1 R_0 + 2\gamma)^2 + \delta^2},$$

where the integral B_0, understood in the sense of the principle value, is due to the contribution of the branch cut c_4. Expression (34) can be simplified if $z_0 = 0$. For $k_1 R_0 \gg \alpha, 2\gamma$ $H_e = H_0 R_0^2 k_1 f(\xi)/2r$, and for $k_1 R_0 \ll \alpha, 2\gamma$ $H_e = -H_0 R_0 f(\xi)/r$ [$f(\xi)$ is determined in (31)]. The integral B_0 can be simplified if $k_1 R_0 \xi \gg 1$, substituting $x = 0$ in the denominator of B_0 and in the function g (except the first term, having a singularity):

$$B_0 = \frac{\alpha b}{2\xi^{3/2}\sqrt{\pi k_1 R_0}}\, {}_1F_1\left(1; \frac{5}{2}, -\alpha\xi\right) - \frac{3(a+b)}{4\xi^{5/2}\sqrt{\pi k_1 R_0}} \tag{35}$$

(${}_1F_1$ is the confluent hypergeometric function). If also $\alpha\xi \gg 1$, (35) is simplified:

$$B_0 = -\frac{3}{4\xi^{5/2}\sqrt{\pi k_1 R_0}}\left(a + \frac{5g_0}{2\xi}\right), \quad g_0 = a + b - \frac{b(\alpha^2 + 4\gamma)}{4\gamma\alpha}. \tag{36}$$

Consequently, for $z_0 \neq 0$ the signal decreases with increasing ξ according to a power law both ahead (Eq. (29)) and behind the front of the elastic wave.

For $\xi < 0$, transforming the integration contour in (33) to the branch cut c_5, and taking into account that the residue at the pole $k = ik_1$, located on the branch cut, vanishes, we obtain

$$H_e = \frac{H_0 R_0^2 k_1}{\pi r}\left\{k_1 R_0 \int_0^1 \frac{x^{3/2} g(x)}{\sqrt{1-x}}\, e^{-k_1 R_0 |\xi| x}\, dx + \right. \tag{37}$$

$$\left. + \frac{z_0}{r}\left[\int_1^{\infty} \frac{x^{3/2} g(x)}{\sqrt{x-1}}\, e^{-k_1 R_0 |\xi| x}\, dx - \text{v.p.}\int_0^{\infty} \frac{x^2 g(x)}{x-1}\, e^{-k_1 R_0 |\xi| x}\, dx\right]\right\}.$$

In the limit $k_1 R_0 |\xi| \gg 1$, $\alpha|\xi| \gg 1$, we find from (37) the asymptotic equation

$$H_e = \frac{H_0}{k_1 r |\xi|^{5/2}}\left\{\frac{3}{4}\sqrt{\frac{k_1 R_0}{\pi}}\left(\frac{5g_0}{2|\xi|} - a\right) + \frac{2z_0}{\pi r\sqrt{|\xi|}}\left(a - \frac{3g_0}{|\xi|}\right)\right\}. \tag{38}$$

We note that for $z_0 = 0$ (38) coincides with (29), taking into account (31). Thus, Eqs. (34)-(38) are in agreement with the analysis provided above.

Consider the terms describing asymptotic diffusion of the magnetic field. Expression (19) must be used for $z_0 = 0$. We carry out the inverse Fourier transform for $k_2 \to 0$ with account of (32). The structure of the given expression is such that the integration contour must be closed in the lower part of the k-plane. Applying the transformations, similarly to what was done above, we obtain

$$H_d = \frac{H_0 R_0^3 k_1 \sqrt{2}}{r^2}\left\{\sqrt{k_1 R_0}\,\mathrm{Re}\left(1 - \frac{\sqrt{k_1 R_0}}{\sqrt{\delta - i(k_1 R_0 + 2\gamma)}}\,e^{-\pi i/4}\right)\times\right. \tag{39}$$

$$\left.\times\frac{A_1}{\sqrt{\delta - 2\gamma i}}\,e^{3\pi i/4} + B_1\right\},$$

$$A_1 = \frac{ci + \alpha b}{[\delta - i(2\gamma + k_1 R_0)]}\exp\left[-r\sqrt{\frac{k_1}{R_0}}\left(\sqrt{\sqrt{\gamma} - \gamma} + \right.\right.$$

$$\left.\left. + i\sqrt{\sqrt{\gamma} + \gamma}\right) - \frac{R_*}{R_0}(2\gamma + i\delta)\right],$$

$$B_1 = \frac{1}{\pi}\,\mathrm{v.p.}\int_0^\infty\left(1 - \frac{1}{\sqrt{1+x}}\right)\frac{g(-x)\cos k_1 r\sqrt{x}}{(1+x)\sqrt{x}}\,e^{-k_1 R_* x}\,dx,$$

where the integral in the principal value sense is related to bypassing the branch cut c_4, and the remaining terms are due to the presence of poles. If the parameter z_0/r is not small, one must use the first term in (23). By means of the inverse Fourier transform we similarly reach the relation

$$H_d = \frac{2H_0 R_0^2 r^3 z_0 k_1}{\pi R^5}\left[B_2 - \pi k_1 R_0\left\{\frac{\alpha b}{\alpha + k_1 R_0}\left(\sin R\sqrt{\frac{\alpha k_1}{R_0}} + \right.\right.\right. \tag{40}$$

$$\left.\left.\left. + \frac{z_0}{r}\cos R\sqrt{\frac{\alpha k_1}{R_0}}\right)e^{-\alpha R_*/R_0} + \mathrm{Re}\,A_1\left(1 + \frac{z_0 i}{r}\right)\right\}\right],$$

$$B_2 = \mathrm{v.p.}\int_0^\infty\left(\cos k_1 R\sqrt{x} + \frac{z_0}{r}\sin k_1 R\sqrt{x}\right)\frac{g(-x)}{x+1}\,e^{-k_1 R_0 x}\,dx,$$

where B_2 is the contribution of the branch cut c_4, and the remaining terms are residues at the poles. At long times, when $k_1 R_* \gg 1$ and $R_*/R_0 \gg \alpha^{-1}, (2\gamma)^{-1}$, the pole terms in (39) and (40) decrease exponentially. The integrals B_1 and B_2 have the asymptotic values

$$B_1 = \frac{e^{-u}}{4\sqrt{\pi}(k_1 R_*)^{3/2}}\left\{a(u-1) + \frac{2R_0 g_0}{R_*}\left(u^2 - u - \frac{3}{4}\right)\right\},\quad u = \frac{k_1 r^2}{4R_*},$$

$$B_2 = a\frac{R_0}{R_*}\left[2\sqrt{w}\,\Phi_1(w) - 1\right] + g_0\frac{R_0^2}{R_*^2}\left[1 - w + 2\sqrt{w}\left(w - \frac{3}{2}\right)\Phi_1(w)\right] -$$

$$- \frac{z_0 R R_0\sqrt{\pi k_1}}{2rR_*^{3/2}}\left[a + g_0\frac{R_0}{R}\left(\frac{3}{2} - w\right)\right]e^{-w},$$

$$\Phi_1 = e^{-w}\int_0^{\sqrt{w}} e^{x^2}\,dx,\quad w = \frac{k_1 R^2}{4R_*}.$$

The asymptotic expressions obtained describe diffusion of magnetic perturbations, while the term B_2 determines, as already noted in investigating relationship (26), the magnetic field of some effective magnetic moment of the diffusing currents.

The analysis carried out above is illustrated by numerical calculations for $z = z_0 = 0$ by Eqs. (34), (37), and (39). We used the approximation of the reduced displacement potential [8] with $P_* = 5\cdot10^8$ Pa, $P_0 = 1.5\cdot10^8$ Pa, $\tau_0 = 0.3$ sec, $\rho c_\ell^2 = 5\cdot10^{10}$ Pa, $c_\ell = 5$ km/sec, $R_0 = 10^2$ m, $\gamma = 0.2$. Figure 4 shows the time evolution of H_z at distance $r = 500$ m for a medium with electric conductivity $\sigma = 1$ S/m, the solid line shows the total field $H_d + H_e$, and the dashed line – the term H_d (39). Figure 5 provides the same dependence for $r = 5$ km and $\sigma = 0.1$ S/m, while in the given case, as shown by the calculations, $H_d \ll H_e$. For geomagnetic field intensity $H_0 = 40$ A/m the signal amplitudes are 10^{-2} and $1.5\cdot10^{-4}$ A/m, respectively, in agreement with the data of [1, 9]. The maximum of both plots corresponds approximately to the input moment at the registration point of the elastic wave. In this case we have a polarity change of the signal. Also characteristic is the presence of electromagnetic indicator of the elastic wave. This feature is illustrated in Fig. 6, where the ξ-de-

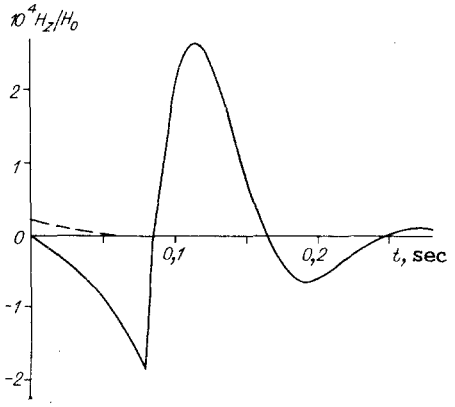

Fig. 4

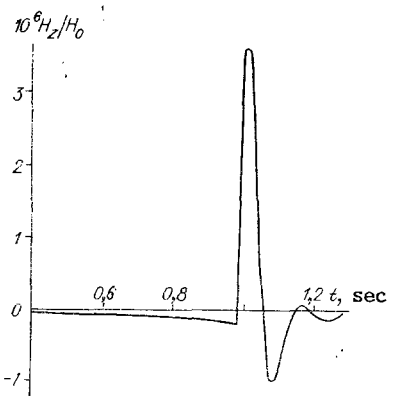

Fig. 5

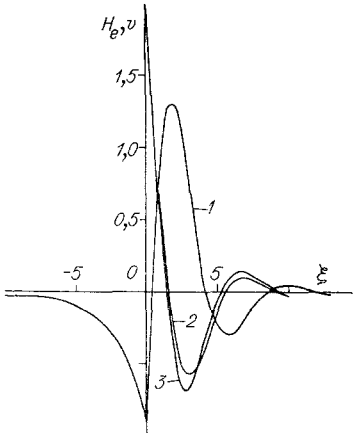

Fig. 6

pendences of the quantities H_e and v are considered. Given are the dimensionless functions $10^3 H_e r/H_0 R_0$ (curve 1, σ = 1 S/m) and $2 \cdot 10^2 vr/c_\ell R_0$ (curves 2 and 3 for r = 500 m and 5 km).

The analysis provided shows that elastic waves accompany geomagnetic perturbations of two types: those localized near the elastic wave front, and perturbations of diffusion character. The existence of an electromagnetic signal, preceding the acoustic (in the near-field zone), is related to the presence of an effective magnetic moment of the currents generated, as well as due to diffusion of the current system. At large distances most substantial are the perturbations propagating with the longitudinal wave. Their amplitude decreases as r^{-1}, and the time dependence is correlated with acoustic quantities, but shifted "in phase." This nature of the signal corresponds to experimental data. The features noted correspond to any shape of seismic source function.

The author is grateful to S. Z. Lunin for a number of useful comments.

LITERATURE CITED

1. S. V. Anisimov, M. B. Gokhberg, et al., "Short-period oscillations of the Earth electromagnetic field during mining explosions," Dokl. Akad. Nauk SSSR, 281, No. 3 (1985).
2. M. B. Gokhberg, I. L. Gufel'd, et al., "Study of perturbations of natural and artificial electromagnetic fields of seismic sources," Izv. Akad. Nauk SSSR, Fiz. Zemli, No. 2 (1987).
3. M. B. Gokhberg, I. L. Gufel'd, et al., "Electromagnetic radiation of a rocky medium under conditions of an explosive load," Dokl. Akad. Nauk SSSR, 295, No. 2 (1987).
4. A. V. Gul'el'mi, "Magnetoelastic waves," Izv. Akad. Nauk SSSR, Fiz. Zemli, No. 7 (1986).
5. A. V. Gul'el'mi, "Excitation of electromagnetic field oscillations by elastic waves in a conducting body," Geomag. Aeronom. 27, No. 3 (1986).
6. L. P. Gorbachev and V. V. Surkov, "Perturbation of an external magnetic field by a Rayleigh surface wave," Magn. Gidrodin., No. 2 (1987).

7. A. V. Gul'el'mi, M. B. Gokhberg, et al., "Induced seismomagnetic sounding of the Earth core," Dokl. Akad. Nauk SSSR, 293, No. 4 (1987).
8. G. Roden, Inelastic Processes in Seismic Waves during Underground Explosions - Nonlinear Wave Processes [Russian translation], Mir, Moscow (1987).
9. O. M. Barsukov and Yu. P. Shovorodkin, "Magnetic observations in the explosive region in Medeo," Izv. Akad. Nauk SSSR, Fiz. Zemli, No. 5 (1969).

DEFORMATION MECHANISM OF A SHOCK RADIATING FRONT DURING ITS MOTION IN A CHANNEL

S. D. Savrov

UDC 533.6.011

Shock front deformation by a powerful shockwave at the walls of a channel filled with inert gas was detected by Shreffler and Christian [1]. A quantitative description of this phenomenon and, even more, a prediction of the conditions for its origination are barely accessible even now. For instance, the detection of such a shock front deformation in a laboratory shock tube turned out to be unexpected [2].

The first attempt at a satisfactory explanation of the front deformation phenomenon was by Taganov [3] on the basis of an analogy between the near-wall curvature of the front and the phenomenon of viscous boundary layer separation. The starting point in this model was the assumption about the presence of a "thermal layer" in front of the shock near the wall heated by radiation. Such a model is in good agreement with experiments in which the "thermal layer" is produced artificially, by heat transmission from a hot burner or a discharge of a metallic wall [4-7]. Under these conditions, the origination of the "thermal layer" is clearly distinct from the conditions of its origination in shock tubes or in a powerful explosion under the surface of the earth. Evaporation of the channel wall is detected ahead of the shock front in a shock tube [2] at quite moderate brightness temperatures (~15 kK). The presence of vapors complicates the problem.

A detailed investigation showed [8] that the vapor layer is thin relative to the channel diameter, and at first glance this permits a bifurcation model that is the development of the scheme presented in [3] to be applied to describe the front deformation.

The flow diagram for such a model is displayed in Fig. 1, where 1 is the tangential surface, 2 is the unperturbed shock front, 3 is the secondary shock front, 4 is the oblique shock, 5 is the boundary of stream collapse, and 6 is the near-wall vapor layer.

The characteristic pattern of bifurcation development in a laboratory shock tube is represented in Fig. 2. The tube diameter is 150 mm, the length of the xenon-filled channel is 1000 mm. The wall material is stainless steel. The initial pressure in the xenon is 13.3 kPa, the shock Mach number is M = 17. At the end of the channel the shock collides with a glass plate which permits determination of its front during observations of the process on a slit photoscanner from the shock endface (Fig. 2, where 1 is the time of shock entrance into the xenon through the separating diaphragm from Lavsan, 2 is the image of the trajectory of the line of intersection of the shock front flanks with the channel walls on the photoscan, 3 is the impact of the front on the glass plate). Despite the clear pattern of the shock front deformation phenomenon, a quantitative analysis of the parameters by the scheme of Fig. 1 is fraught with difficulties.

It is seen from additional experiments that under the same initial conditions in a long channel (3 m) propagation of the front deformation to the channel axis ceases after shock traversal of a distance of 6-8 calibers of the tube channel. The deformed shock front surface emerges into the stationary mode. Such a mode had not been assumed earlier in the scheme in Fig. 1. The shock front deformation in [1, 4-10] was nonstationary.

Moscow. Translated from Zhurnal Prikladnoi Mekhaniki i Tekhnicheskoi Fiziki, No. 5, pp. 30-33, September-October, 1989. Original article submitted May 4, 1988.

 0021-8944/89/3005-0696$12.50